Talanta 149 (2016) 53–61

Contents lists available at ScienceDirect

Talanta

journal homepage: www.elsevier.com/locate/talanta

Development and validation of a laser-induced breakdown spectroscopic method for ultra-trace determination of Cu, Mn, Cd and Pb metals in aqueous droplets after drying

Nadir Aras, Şerife Yalçın *

İzmir Institute of Technology, Faculty of Science, Chemistry Department, 35430 İzmir, Turkey

ARTICLE INFO

Article history:
Received 23 September 2015
Received in revised form
6 November 2015
Accepted 12 November 2015
Available online 14 November 2015

Keywords:
Laser-induced breakdown spectroscopy
Liquid droplet analysis
Oxidized silicon wafer substrate ($Si+SiO_2$)

ABSTRACT

The present study reports a fast and accurate methodology for laser-induced breakdown spectroscopic, LIBS, analysis of aqueous samples for environmental monitoring purposes. This methodology has two important attributes: one is the use of a 300 nm oxide coated silicon wafer substrate ($Si+SiO_2$) for the first time for manual injection of 0.5 microliter aqueous metal solutions, and two is the use of high energy laser pulses focused outside the minimum focus position of a plano convex lens at which relatively large laser beam spot covers the entire droplet area for plasma formation. Optimization of instrumental LIBS parameters like detector delay time, gate width and laser energy has been performed to maximize atomic emission signal of target analytes; Cu, Mn, Cd and Pb. Under the optimal conditions, calibration curves were constructed and enhancements in the LIBS emission signal were obtained compared to the results of similar studies given in the literature. The analytical capability of the LIBS technique in liquid analysis has been improved. Absolute detection limits of 1.3 pg Cu, 3.3 pg Mn, 79 pg Cd and 48 pg Pb in 0.5 microliter volume of droplets were obtained from single shot analysis of five sequential droplets. The applicability of the proposed methodology to real water samples was tested on the Certified Reference Material, Trace Metals in Drinking Water, CRM-TMDW and on ICP multi-element standard samples. The accuracy of the method was found at a level of minimum 92% with relative standard deviations of at most 20%. Results suggest that 300 nm oxide coated silicon wafer has an excellent potential to be used as a substrate for direct analysis of contaminants in water supplies by LIBS and further research, development and engineering will increase the performance and applicability of the methodology.

1. Introduction

Laser-induced breakdown spectroscopy [1–2] is among the most popular techniques due to its remarkable features like non-invasiveness, micro-local analysis ability, high speed, portability and multi-element capability. Recently, studies on ultra-trace level detection by LIBS is increasing, especially with recent applications of the technique in environmental, biochemical and nuclear technology that necessitates in-situ, fast and real time analysis with high sensitivity. While LIBS offers simple and versatile measurement for the analysis of solids with an acceptable precision, direct liquid analysis by LIBS has several experimental difficulties experienced during analysis like, splashing, bubbling, self focussing that reduces the analytical capability of the technique. Therefore, liquid analysis by LIBS has required some special methodologies/ pretreatment steps to be performed before direct analysis of the samples.

Plasma formation on flowing jet liquids [3–5], inside bubbles [6], on liquid droplets [7–8], on aerosols formed by nebulization [9,10] or by electro-spray ionization [11,12], on samples in which physical conditions are changed by freezing [13,14] or by chemical derivatization [15–18], liquids adsorbed on solid substrates [19–23] or on sol–gels [24] and use of sequential laser pulses [25–29] are some of the efforts devoted in the last decade to increase the analytical capability of the LIBS technique for liquids analysis. Also, filtration based approaches, collection of the suspended particles like pollen, bacteria, fungi and viruses on filters enabled analysis of biological materials in water [30]. Most of the approaches on the current aqueous LIBS research are reviewed in a recent article [31] for environmental monitoring of water quality.

The transfer of the analyte from the liquid to solid phase by solid phase extraction/microextraction techniques, (SPE/SPME) [32,33], is among the most studied pretreatment approach for liquid LIBS studies. Recently, hyphenation of LIBS detection with

* Corresponding author.
E-mail address: serifeyalcin@iyte.edu.tr (Ş. Yalçın).

http://dx.doi.org/10.1016/j.talanta.2015.11.031
0039-9140/

common analytical sample enrichment methodologies like liquid phase micro-extraction (LPME), dispersive liquid–liquid micro-extraction (DLLME) and single drop micro-extraction (SDME) [34–37] are used to improve sensitivity and detection capability of the LIBS technique in liquids analysis. The precipitation of the analyte followed by membrane separation approach [38] also provided dramatic enhancements in detection limits of some elements. In most of these microextraction based analyte enrichment methodologies, the final extract may be in a few microliters volume and is suitable for droplet analysis by LIBS on account of its ability to perform analysis on micrometers size materials.

LIBS analysis of evaporated droplets, after preconcentration procedures applied, on various solid substrates is recently used by several groups. Shi et. al. [33] used a 3D anodic aluminum oxide porous membrane (AAOPM) as a substrate for loading 100 microliters of analyte solution and performed LIBS analysis after drying. They observed strong enhencement in LIBS signals and explained this enhancement with the formation of strong metal–oxygen bond between hydroxyl groups and metal ions existed on the surface of the substrate, larger contact area between the matrix and analytes and also efficient coupling of a laser beam with the material due to special nano-channel distribution of the substrate. The LODs were at the level of sub-ppm solution concentrations as 0.18, 0.12, 0.081 and 0.11 μg mL^{-1} (ppm), for Cu, Ag, Pb and Cr elements, respectively.

Aluminum, in the form of thin foil and as a metallic alloy, was used as a sample loading substrate for droplet analysis, after liquid–liquid extraction procedures with extracting solvents of; 10% Triton X-114 [34]; ammoniumpyrolidinedithiocarbamate (APDC)-toluene [35,36], and 8-hydroxyquinoline (8-HQ)-1-undecanol [37] were used. For these cases, LIBS analyses were performed on droplets dried on the aluminum substrate either at room temperature or on a hot plate. Aguirre et.al [34] reported that, with direct analysis of suspended droplets at the tip of a microsyringe, manganese emission lines were undetectable at concentrations lower than 0.2%, however, dry microdroplet analysis of manganese, extracted in 10 % Triton matrix, on aluminum metal substrate resulted with enhancement in Mn signals. Recently, the same group has also applied single drop microextraction (SDME) [35] and dispersive liquid–liquid extraction (DLLME) [36] methodologies for preconcentration, using toluene and tetrachloromethane as extraction solvents of Cr, Mn, Ni, Cu and Zn analytes in the form of (APDC) complexes. Microliters volume of analyte enriched solvents were converted into solid by drying on the heated aluminum foil surface prior to LIBS detection. The results of the comparative LIBS measurements of SDME methodology indicate improvements of 2.3 fold in sensitivity and 2.5 fold in LODs compared to the ones obtained by direct LIBS analysis of the liquid samples. Authors also find DLLME methodology, performed in a few microliters of an organic extractant CCl_4, is twice more efficient and faster than SDME, with 5.0 and 4.5 fold enhancements in sensitivity and LOD values, respectively. Another DLLME study based on the use of 8-hydroxyquinoline and 1-undecanol as extracting solutions for the determination of V and Mo was performed by De Jesus et. al [37]. Analysis of 10 μL of organic solvent after evaporation on aluminum foil substrate on a hot plate resulted with detection limits of 30 μg L^{-1} for Mo and 5 μg L^{-1} for V.

Direct analysis of Cs in the droplets of biological fluid samples, urine and blood serum, was also performed [39]. They used Zn metallic substrate by forming small pockets to confine the droplets and create a layer of solid deposit after drying. By using multiple standard addition method, quantitative determination of 6 μg mL^{-1} Cs in the urine and 27 μg mL^{-1} Cs in the blood serum samples were achieved.

As is shown in the literature by several groups, LIBS analysis of evaporated droplets on metallic substrates, after preconcentration procedures, presents a simple and sensitive methodology and provides better analytical figures of merit compared to direct liquid analysis by LIBS. Also, matrix conversion and analyte preconcentration approaches are advantageous in terms of small sample volume involved, however, use of several chemicals in the extraction process may result with serious interference effect in spectral analysis. In addition, inhomogeneous lateral distribution of the solid deposits dried on substrates requires carefull sampling of the droplets by focussed laser pulses.

Here, we present a different substrate and a different sampling geometry to improve the analytical capability of the LIBS technique in liquid droplet analysis. For this purpose 0.5 μL droplets of Cu, Mn, Cd and Pb analyte solutions were placed on 300 nm oxide grown silicon wafer substrate ($Si+SiO_2$) and subjected to LIBS analysis after drying. For LIBS analysis, energetic laser pulses, focused to a relatively large spot outside the minimum focus condition, were used to form a more stable and homogeneous plasma and enhancements in the detection limits were achieved. We describe the methodology and demonstrate the results obtained from the LIBS analysis of dried droplets in the following sections.

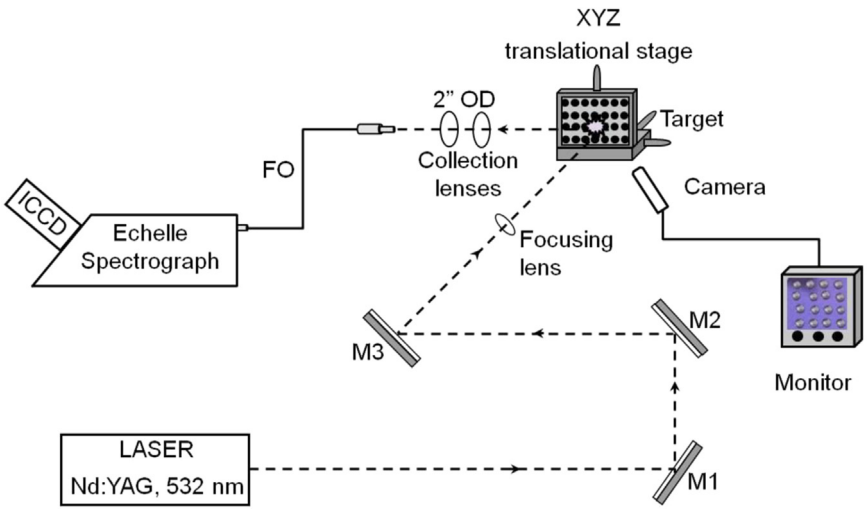

Fig. 1. Experimental LIBS setup. M1, M2 and M3: reflecting laser mirrors, FO: fiber optic cable, ICCD: Intensified Charge Coupled Detector.

Table 1
Optimum instrumental LIBS parameters including delay time, gate time and laser pulse energy for Cu, Mn, Cd and Pb.

Elements	Emission Line (nm)	t_d (μs)	t_g (μs)	Pulse energy (mJ)
Cu	324.87	1.75	500	200
Mn	403.08	1.00	750	200
Cd	226.50	0.75	500	200
Pb	405.78	2.00	500	200

2. Experimental

2.1. LIBS instrumentation

LIBS system used in this work, schematically shown in Fig. 1, was constructed from its commercially available parts. A Q-switched Nd:YAG laser source (Quanta-Ray Lab-170, Spectra Physics) has been operated at its second harmonic, 532 nm, with 10 ns duration time. The laser beam was directed to the target by using 532 nm reflective mirrors (1" OD, coated, 532 nm reflective, New Focus), and focused onto the sample surface via 17.5 cm focal length plano convex lens from 15 cm distance to the sample. At this distance, laser beam spot size was around 1.3 mm in diameter, which is large enough to cover the entire droplet area for ablation from a single laser shot. The average irradiance value of 1.51 GW cm−2 was obtained under these conditions.

Laser pulse energy was measured by a power meter (PE50BB-DIF-V2, Nova II, Ophir). Samples were mounted on an XYZ-translation stage (New Focus) to provide fresh spots during sampling. The sampling position on the target with respect to the laser beam was controlled with a camera and a monitor system (Honeywell, HMM9/HMM9X). A fiber optic cable with 450 micrometers core diameter was used to carry plasma emission onto the entrance slit of an echelle spectrograph (Mechelle 5000, Andor Inc.) equipped with an intensified charged coupled device (ICCD) (iStar DH734, Andor Inc.). The spectrograph and detection system spectral range is between 200 and 850 nm with 0.08 nm resolution at 400 nm.

2.2. Reagents and sample preparation

Thermally oxidized silicon wafer with 300 nm thick oxide layer ($Si+SiO_2$ wet, Nanografi, Ankara, Turkey) was used as a substrate without pretreatment. Aqueous calibration standards were prepared by suitable dilution of 1000 mg L^{-1} single element standard solutions of Cu, Mn, Cd and Pb (High-Purity Standards) with ultrapure water. Certified Reference Material, Trace Metals in Drinking Water, CRM-TMDW-A (High-Purity Standards) and ICP Multielement Standard (AccuStandard) were used for validation experiments after appropriate dilutions.

Aqueous metal solutions of 0.5 μL target analytes (Cu, Mn, Cd and Pb) were manually deposited on (1 × 1 cm) precut $Si+SiO_2$ substrate with a micropipette dispenser. These droplets were then evaporated to dryness at room temperature for about 5 minutes and converted from liquid to solid. Finally, $Si+SiO_2$ substrate with dry residues of target analyte was placed on the translational stage for LIBS analysis.

3. Results and discussion

3.1. Optimization of instrumental parameters

In order to achieve the best analytical performance of a LIBS system, signal intensity should be maximized at the analytical line of interest by careful selection of the instrumental parameters. Therefore, optimization of instrumental LIBS parameters like detector delay time, gate width and laser energy has been performed for each element, separately.

Laser pulse energy is one of the critical factors that affects the plasma formation in LIBS measurements. Some of the important parameters including plasma temperature, ablation characteristics and extent of ionization are affected by the magnitude of the laser pulse energy. The optical geometry used in this study focuses the laser beam to a relatively large spot, therefore higher pulse energies are required to initiate the breakdown on dried droplets. Energy dependence of signal intensity was investigated between 60 mJ and 240 mJ pulse energies. Most prominent emission lines of Cu (I) 324.75 nm, Mn (I) 403.08 nm, Cd (II) 226.50 nm and Pb (I) 405.78 nm were monitored using 1 mg L^{-1} aqueous solutions of each target element. Generally, a linear increase in signal intensity with respect to an increase in pulse energy was observed, however, at energies higher than 200 mJ, measurements suffered from the high noise signals. Therefore, laser pulse energy of 200 mJ was selected as the optimal value for each element analyzed. Selection of optimum detector delay time with respect to incoming laser pulse, t_d, and gate window, t_g, were carefully studied to maximize the emission line of each element, separately. Experimental parameters obtained from the optimization studies are listed in Table 1, below.

3.2. Focusing geometry

The actual energy density at the target is very much dependent on the particular focusing conditions and hence laser beam spot size. The optical and geometrical focussing conditions has some important effect on plasma size, shape and also the spatial locations of each element present in the plasma, and has been studied for other LIBS applications [40,41]. LIBS measurements are normally performed by tightly focusing the laser beam perpendicular to the target surface. Maximum irradiance is obtained with minimum focal area of the laser spot. At high irradiances, air breakdown occur in front of the focal point of a lens. This hard focusing condition may result with observation of emissions from the dust particles present in the medium or scattering of the laser beam by the aerosols generated in the previous ablation process. Therefore the analytical performance of the technique is reduced. This problem can be eliminated by keeping the distance between the focusing lens and the target a little shorter than the focal length of the lens. In this condition, a very shallow focusing of the laser beam occurs, spot size becomes larger and interaction area with the target increases. With the expense of using high energy laser pulses for plasma formation, plasma size becomes larger and the LIBS signal intensity increases.

In order to get benefits of this optical geometry, droplet analyses were performed at the out-of-focus condition. The schematic diagram of the laser beam focusing condition used in this study is described in Fig. 2. The substrate was placed at 2.5 cm inside the focal point position of a 17.5 cm plano convex lens and the laser beam size was around 1.3 mm in diameter. Each laser pulse was large enough to cover a single droplet for ablation. Experimental results of the beam size effect at the minimum focus and out-of-focus conditions in terms of *S*/*N* ratio and %RSD are given in the Section 3.3 below, for better understanding, after the morphology of the craters are discussed.

3.3. Morphology of the craters

Droplet shape and crater morphology of laser ablated ($Si+SiO_2$) surfaces were investigated by scanning electron microscope (SEM) pictures. Fig. 3(a–c) shows, SEM images of; a bare ($Si+SiO_2$) surface, a dried droplet of copper solution on ($Si+SiO_2$) substrate and a crater of a laser ablated droplet produced from a single laser

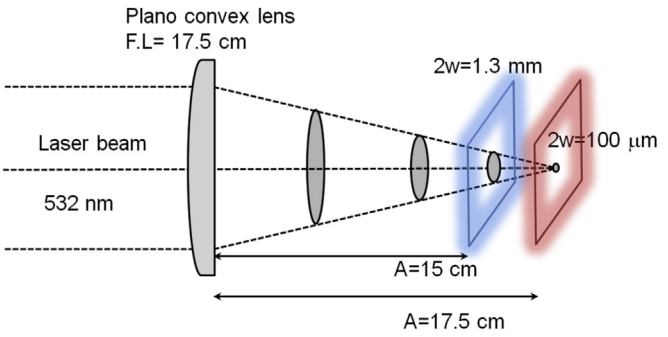

Fig. 2. Schematic diagram for focusing of the laser beam for dry droplet analysis. A: focusing lens distance to the target, F.L: focal length of a plano convex lens, 2w: laser beam diameter.

pulse of 200 mJ energy at the out of focus condition. SEM pictures of a single droplet area sampled with tightly focused laser pulses are also shown in Fig. 3(d and e).

Surface structure of 300 nm oxide grown silicon wafer ($Si+SiO_2$) is given in Fig. 3(a). Weight percentages of 67% silicon and 33% oxygen were obtained from EDX measurements. It can be seen that the majority of the SiO_2 particles are around 30–40 nm in size however, bigger particles of around 400 nm size due to aggregation of small particles are clearly observed. It is belived that, this roughness on SiO_2 surface provides a much higher surface area for immobilization of metal ions in liquid droplets compared to unoxidized silicon wafer surface. SEM picture of a 0.5 μL droplet given in Fig. 3(b) shows that the droplet dries nicely in a circular shape with a millimeter size diameter but irregularly distributed copper crystals are apparent. Sampling of this droplet area with multiples of tightly focused laser pulses produces highly varying LIBS signals from one to another laser shot and necesitates a careful sampling procedure to be applied. A crater formed with a laser beam size as large as the droplet size, at the out-of-focus condition, is shown in Fig. 3(c). It is clearly seen that the laser beam covers the whole droplet area for ablation and exhibits almost uniform ablation throughout the droplet area. Profilometric measurements of ablated craters reveals an average of 300 nm depth, in which the depth variation is around 30%. The presence of no remarkable LIBS signal from the second laser pulse on the same sampling spot indicates that the sample deposited stays on/inside the 300 nm thick SiO_2 layer of silicon wafer and has been analyzed within the first laser shot.

Craters of 16 sequential sampling in a single droplet area with tightly focused laser pulses are shown in Fig. 3(d). In the enlarged view of one of these craters, Fig. 3(e), surface explosion with debris around the edges of the crater and contamination of the craters from the subsequent laser pulses are clearly observed. Instead of making several samplings with tightly focussed laser beam at different locations of a single droplet, as is shown in the literature by Aguirre et al. in their several work [34–36], sampling the whole droplet area in a single laser shot may eliminates shot to shot variation of the signal due to inhomogeneous deposition of the analyte. In addition, sample losses between the samplings may also be prevented. Therefore, increased signal intensity is obtained.

In order to better understand the beam size effect to support the signal intensity enhancement at the out-of-focus condition, experiments at the minimum focus (2w=0.1 mm) and out-of-focus (2w=1.3 mm) conditions were performed. For experiments at the minimum focus, 5 replicate droplets of 0.5 μL copper solutions were placed on a ($Si+SiO_2$) surface by a micropipette. After drying, each droplet area was raster scanned in 16 different positions (4×4) by focused laser pulses of 100 micrometer diameter and 5 mJ pulse energy, for LIBS analysis. At each sampling position of a single droplet, 5 repetitive laser pulses were acquired and stored separately for statistical analysis. Out-of-focus experiments were performed by sampling 20 separate droplets on ($Si+SiO_2$) substrate with single laser pulses of 1.3 mm size and 200 mJ pulse energy. For comparison, LIBS emission signals at the minimum focus and out of focus conditions, for the most prominent lines of Cu (I) at 324.75 and 327.40 nm are given in Fig. 4. Data at the minimum focus, presented as a dashed line in the figure is from the summation of 16 different samplings in one droplet, each is the accumulation of 5 repetitive pulses whereas, out-of-focus condition data, solid line, is the average of 20 single pulse samplings. As can be seen from the Fig. 4, Cu (I) signal at 324.75 nm

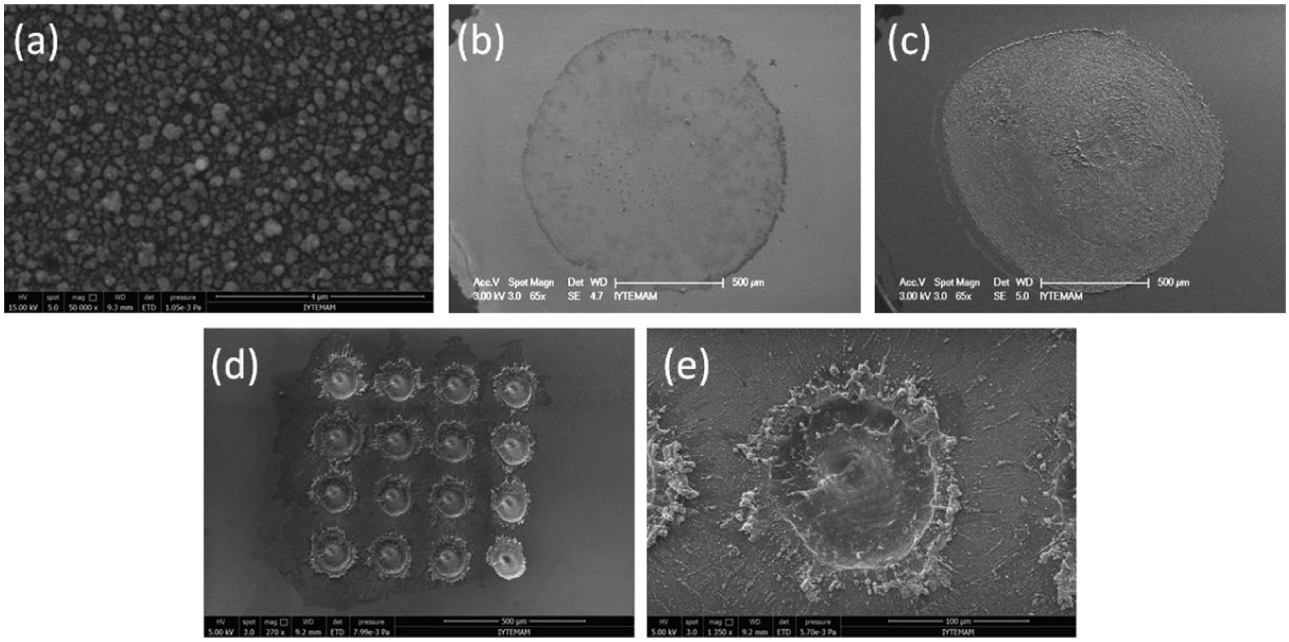

Fig. 3. SEM images of; (a) a bare ($Si+SiO_2$) surface, (b) 0.5 μL dried droplet of 1 mg L^{-1} copper solution on ($Si+SiO_2$) surface, (c) a crater of a laser ablated droplet by a 200 mJ single laser pulse on ($Si+SiO_2$) surface at the out of focus condition, (d) 16 sequential sampling in a single droplet area with tightly focussed laser pulses and (e) the enlarged view of one of the craters given in (d).

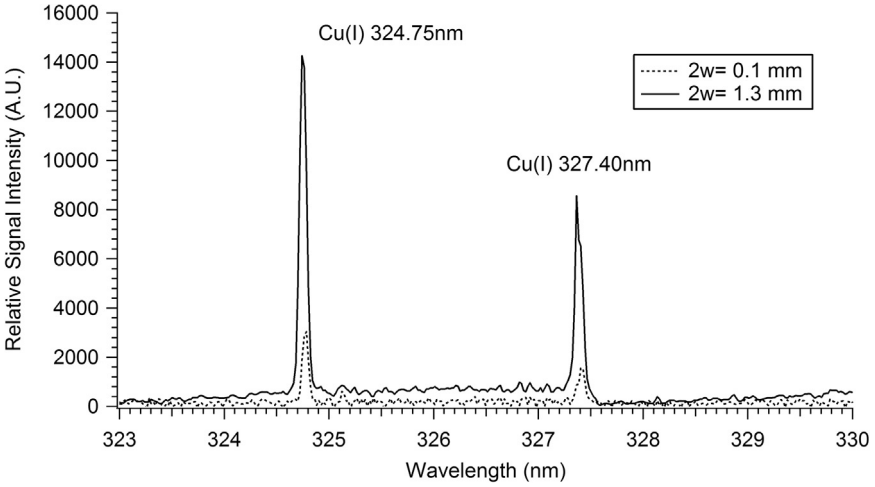

Fig. 4. LIBS emission signals at the minimum focus and out of focus conditions for the most prominent lines of Cu (I) at 324.75 and 327.40 nm. Data at the minimum focus condition, presented as a dashed line in the figure, is from the summation of 16 different samplings, each is the accumulation of 5 repetitive shots. Out-of-focus data, solid line, is the average of 20 single shot samplings. Experiments were performed under 1.51 GW cm^{-2} and 6.36 GW cm^{-2} laser irradiances at the minimum focus and out-of-focus conditions, respectively.

enhances 6.5 fold compared to the one at the minimum focus condition.

LIBS emission signal for Cu (I) line at 324.75 nm was also analyzed in terms of *S*/*N* and %RSD. Calculations were performed over 16 samplings for each 5 droplets ($16 \times 5 = 80$ total) at the minimum focus condition and 20 single shot sampling at the out-of-focus configuration. Here, the signal is defined as the peak area of the background subtracted Cu (I) line, and the noise is three times standard deviation of the background. Background is calculated from the region of the spectrum close to the analytical line of interest. Statistical analysis results, given in Table 2. below, suggests more than 7 times enhancement in *S*/*N* for the experiments performed at the out-of-focus condition compared to the ones at the minimum focus condition. Also, relative standard deviation of *S*/*N* values improves from 28% to 16%, almost twice, at the out-of-focus condition. Analysis of 5 droplets out of 20, at the out-of-focal point configuration was yielded similar *S*/*N* and RSD values with the ones obtained from the analysis of 20 droplets.

3.4. LIBS analysis of Cu, Mn, Cd, and Pb droplets on ($Si+SiO_2$) substrate

Laser-induced breakdown spectroscopic analysis of Cu, Mn, Cd, and Pb droplets on ($Si+SiO_2$) substrate was carried out at the out-of-focus configuration and under the optimum instrumental conditions. For this purpose, 0.5 μL aqueous solutions of target analyte were transferred to ($Si+SiO_2$) substrate. After drying, droplet diameters were about 1–1.2 mm and the laser beam focussed at 2.5 cm away from the focal point position was covering the entire droplet area to ablate in a single laser shot.

Representative LIBS spectra obtained from Cu, Mn, Cd and Pb droplets under optimum experimental conditions are shown in Fig. 5. The spectra between 200 nm and 850 nm spectral range were obtained from the 0.5 μL of 1 mg/L analyte concentration of each element. That corresponds to detection of 500 pg Cu, Mn Cd and Pb in a single laser shot with high sensitivity. Insets in each spectrum, are the most representative atomic emission line profiles used for quantitative LIBS analysis. In each spectra, strong emission lines of neutral Si(I) at 263.13 nm, 288.15 nm, 390.55 nm and ionic Ca(II) emission lines at 393.37 nm, 396.85 nm and neutral Ca(I) 422.67 nm, neutral Na(I) at 589.0 nm and 589.6 nm, ionic Mg(II) at 279.55 nm and 280.27 nm were observed. Presence of Na, Ca, Mg lines along with Si may represent the presence of impurities in ($Si+SiO_2$) substrate.

Table 2
Statistical analysis results of Cu (I) signal at 324.7 nm from the experiments at the minimum focus and out-of-focus configurations. Analyte concentration of 1 mg L^{-1} was used. A: focusing lens distance to the target, 2w: laser beam diameter, L.E: Laser pulse energy, I: Irradiance.

	Minimum focal point	Out-of-focal point	
S/*N*	29[a]	205[b]	198[c]
% RSD	28	16	13
A (cm)	17.5	15.0	
2w (μm)	100	1300	
L.E (mJ)	5	200	
I (GW cm^{-2})	6.36	1.51	

[a] From the analysis of 5 droplets each is the sum of 16 samplings, each sampling is accumulation of 5 repetitive laser pulses.
[b] From the analysis of 20 droplet.
[c] From the analysis of 5 droplets out of 20.

3.5. Quantitative analysis of dry droplets by LIBS

3.5.1. Growth curves and analytical figures of merit

In order to investigate the quantitative LIBS analysis of Cu, Mn, Cd and Pb droplets dried on ($Si+SiO_2$) substrate, and to determine the analytical performance characteristics of the methodology proposed, calibration curves were constructed from a set of calibration standards with known concentrations. Data is obtained from the single shot measurements of 5 separate droplets for each different concentrations of the analyte. Relative signal intensity values were obtained from the peak heights of atomic emission lines after background emission was subtracted. Calibration graphs constructed from their respective LIBS measurements are shown in Fig. 6.

Calibration curves demonstrate a linear behavior over a range of concentrations from 10 ng/mL (ppb) to 10 μg/mL (ppm) with R^2 values of 0.99, 0.97, 0.95 and 0.98 for Cu, Mn, Cd and Pb respectively. Limit of detection (LOD) was determined for each element according to the IUPAC definition, with 95% confidence level, $LOD = 3\sigma_{BG}/m$, where σ_{BG} is the standard deviation of the background and m is the slope of the calibration curve. A list of the LOD values obtained from the calibration curves constructed for Cu, Mn, Cd and Pb are given in Table 3. along with the relevant literature values.

LOD values are given in concentration units of ppb (ng/mL), being as 2.5 ng/mL for Cu, 6.7 ng/mL for Mn, 158 ng/mL for Cd and

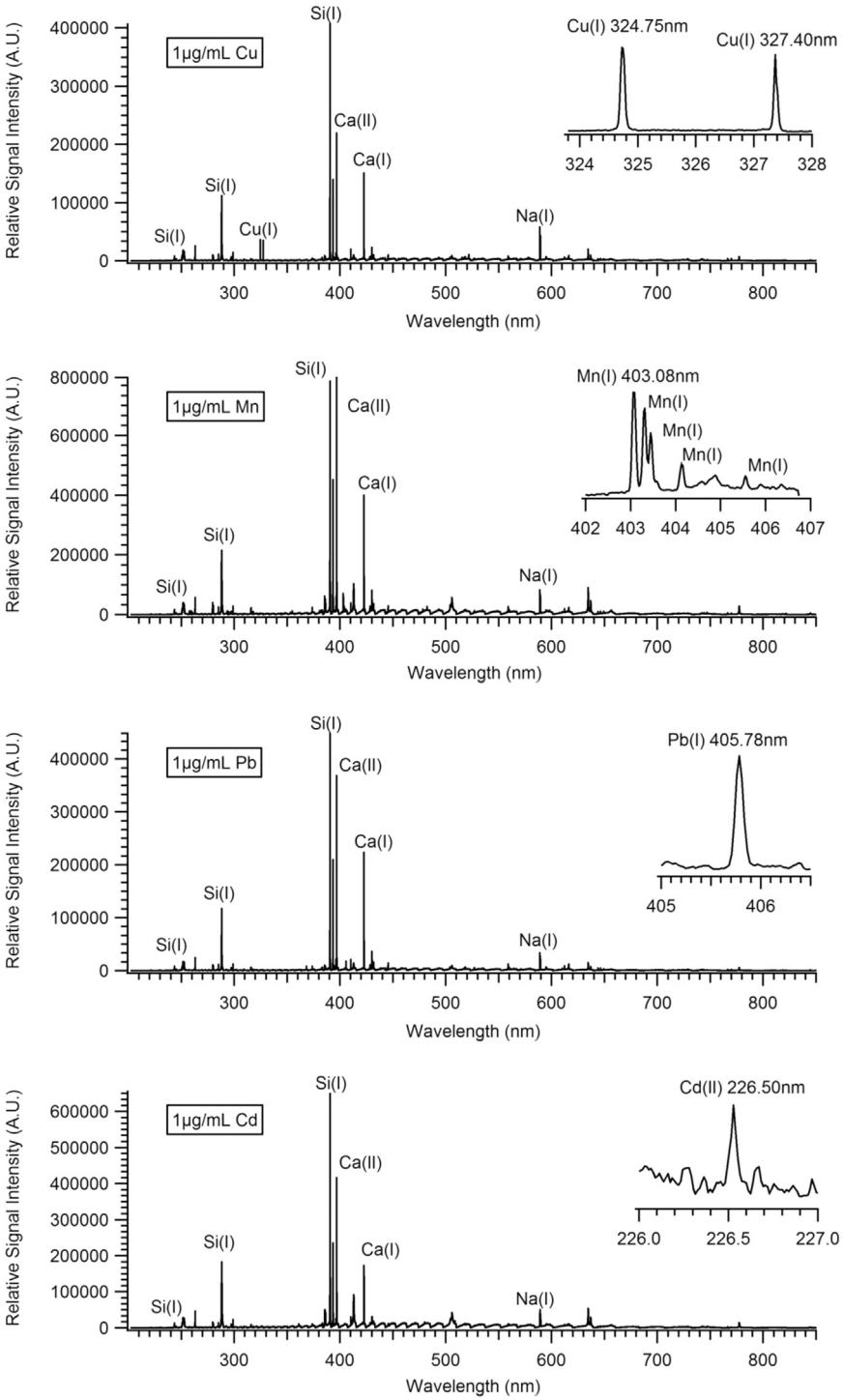

Fig. 5. Representative LIBS spectra obtained from dried droplet residues of 0.5 μL, 1 μg/mL Cu, Mn, Pb and Cd samples under their optimum instrumental conditions, given in Table 1.

95 ng/mL for Pb. Considering that 0.5 μL of droplet volume was used for analysis, these LODs correspond to absolute detection of 1.3 pg Cu, 3.3 pg Mn, 79 pg Cd and 48 pg Pb. When these results are compared with the literature values listed in Table 3., they are at least one to three orders of magnitude lower, from element to element, than the ones obtained by direct liquid analysis in water or on ice [14,34]. To the best of our knowledge, especially for Cd and Pb, this is the only study that sub-ppm detection limits are obtained from the direct analysis of liquids. When the literature results that incorporate enrichment strategies followed by the use of aluminum substrate [34–36] are compared, the present results are still at least an order of magnitude lower. Enhancement factors of 9 and 21 for Cu, and 7 and 45 for Mn were observed with respect to DLLE and SDME approaches. It should be mentioned here that, unless the absolute amounts are expressed, comparing LOD results of different studies may not be correct, due to the use of different focusing geometry, experimental conditions and statistical considerations during data analysis.

It is also worth to indicate that, the approach presented in this study does not contain any laborious, prone to contamination and

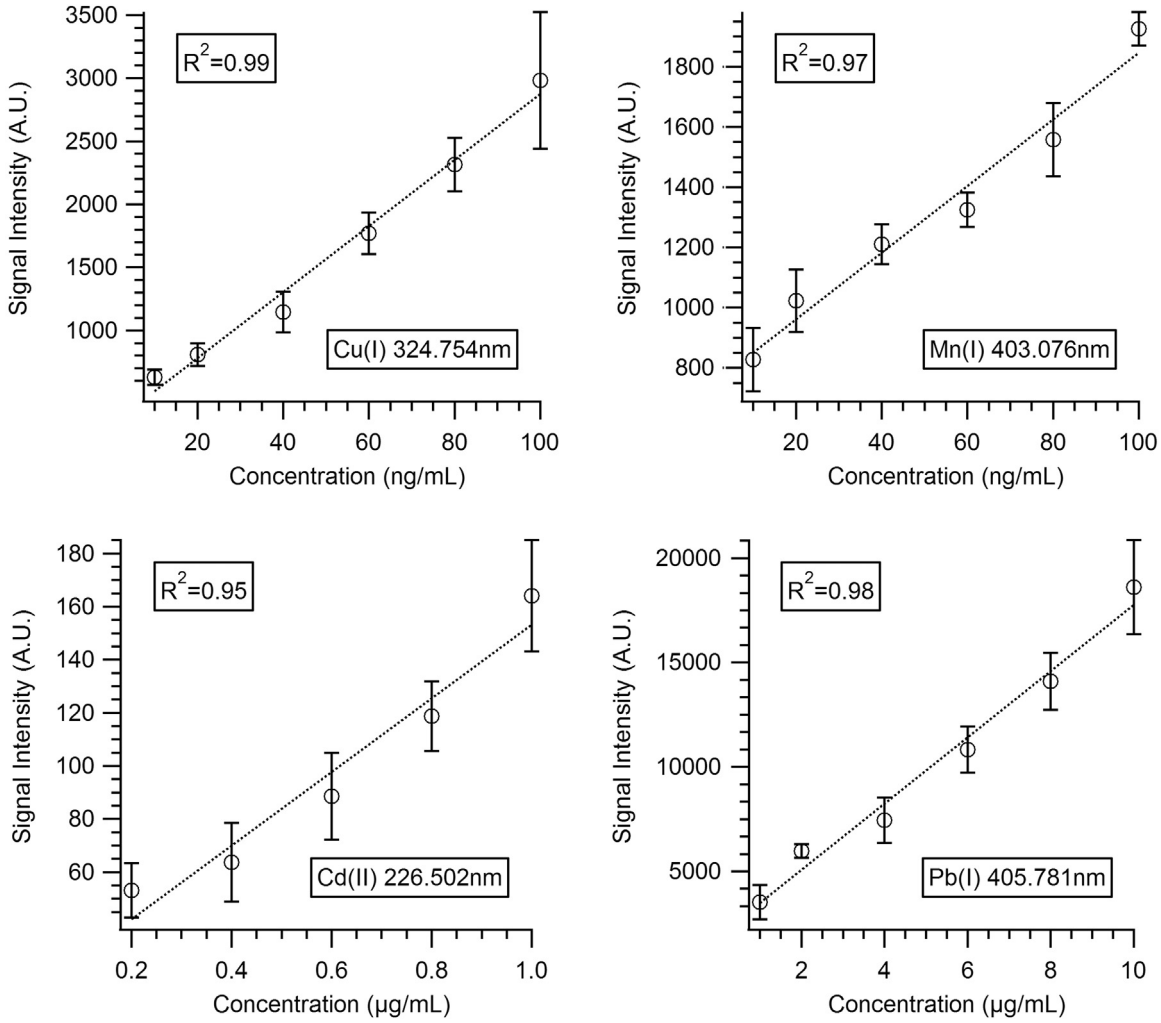

Fig. 6. Calibration graphs for Mn (I) 403.076 nm, Cd (II) 226.502 nm, Cu (I) 324.754 nm and Pb (I) 405.78 nm between concentration range of (10–100 ng/mL) for Cu and Mn, and (0.1–1 μg/mL) for Cd and (1–10 μg/mL) for Pb. Instrumental conditions are listed in Table 1.

costly preconcentration/enrichment steps that involve use of several chemicals. Instead, direct placement of analyte droplets on the ($Si+SiO_2$) substrate for LIBS analysis was performed. Therefore, it is much simpler, fast and less costly methodology than other liquid to solid conversion techniques that employ chemical enrichment processes.

The enhancements observed in signal intensities and better LODs may be attributed to the physical/chemical properties of the oxide grown silicon wafer ($Si+SiO_2$) substrate in which a higher surface area is available for immobilization of metal ions. Moreover, use of a relatively larger laser spot size at the out-of-focus condition provides increased interaction area with the target therefore, larger plasma size and hence increased signal intensities are observed. The substrate effect in LIBS analysis of micro droplets is first mentioned by Aguirre et al., in their article where aluminum was used as a substrate, and coined as surface enhanced LIBS, SENLIBS [34]. Currently, no comprehensive research based on investigating the substrate effect in droplet analysis is present. While we report here the results with ($Si+SiO_2$) substrate, use of different substrates for liquid analysis is an ongoing research in our laboratory.

3.5.2. Analysis of certified reference material (method validation)

In order to validate the applicability of the proposed methodology to real water analysis, a certified reference water sample, Trace Metals in Drinking Water, CRM-TMDW and an ICP multi-element standard sample, ICP-MES that contain 24 elements were used. Analyses were performed by sampling five replicate droplets of the reference material for each element, separately, under their optimum instrumental conditions. Then, the average of these five measurements was run through the equation obtained from the calibration curves to determine analyte concentration and error of measurements, for each element. Accuracy values were calculated from the use of certified and determined values of each element.

Analysis of CRM-TMDW reference sample was performed without dilution due to low concentration levels of the elements present. Cu and Mn analyses were performed with 98% and 92% accuracy, however, the concentration levels for Cd and Pb were lower than the detection limit of the technique and Cd and Pb could not be analyzed in drinking water reference samples. Instead, for Cd and Pb analysis, ICP-MES standard solution was used after dilution, 10 times for Pb and 50 times for Cd. Table 4. lists the certified and experimentally determined Cu, Mn, Cd and Pb concentrations from the reference materials. Accuracy values for Cd and Pb are higher than 100% being as 107.8% for Cd and 115.1% for Pb. That could be associated with dilution errors and also reduced matrix effect as a result of dilution. Precision of the measurements, expressed as %RSD, are in the range commonly observed in most LIBS analyses, as between 12.4% and 20.7%.

Table 3
Limit of detection (LOD) values for analysis of Cu, Mn, Cd and Pb droplets related with literature results.

Wavelength (nm)	LOD (ng/mL)	Reference number	Methodology used
Cu (I) 324.75	*2.5*	*This study*	
	2.59	[38]	Precipitation/membrane separation
	15	[32]	PVC-membrane filter
	180	[33]	AAOPM membrane filter
	54	[35]	SDME/droplet on Al foil substrate
	23	[36]	DLLE/ droplet on Al foil substrate
	2300	[14]	On ice
	9600	[14]	In water
Mn (I) 403.08	*6.7*	*This study*	
	6000	[34]	LLE-droplet on aluminum substrate
	10.85	[23]	DSPME-Nano Graphite adsorbent
	0.958	[38]	Precipitation/membrane separation
	301	[35]	SDME/droplet on Al foil substrate
	49	[36]	DLLE/droplet on Al foil substrate
Cd(II) 226.50	*158*	*This study*	
	1400	[14]	On ice
	7100	[14]	In water
Pb (I) 405.78	*95*	*This study*	
	81	[33]	AAOPM membrane filter
	1300	[14]	On ice
	12500	[14]	In water

Table 4
Analysis of CRM and ICP-MES reference material.

Element	Certified value (ng/mL)	Found value (ng/mL)	Accuracy (%)	Precision (% RSD)
Cu	$20.0 \pm 0.2^{*}$	19.7	98.4	12.4
Mn	$40.0 \pm 0.4^{*}$	36.9	92.3	14.9
Cd	25000**	26940	107.8	20.7
Pb	50000**	57540	115.1	14.5

* From CRM-TMDW-A reference sample.
** From ICP-MES sample before dilution. Cd samples were diluted by 50 times and Pb samples were diluted by 10.

4. Conclusions

A laser induced breakdown spectroscopic method based on direct analysis of liquid droplets after drying on a novel ($Si+SiO_2$) substrate at room temperature was developed. 500 nL volume of Cu, Cd, Pb and Mn droplets were subjected to high energy laser pulses focused on the sample surface, outside the minimum focus position of a 17.5 cm focal length plano convex lens, from 15 cm distance to the sample. At this position, the laser beam with 1.3 mm beam size was covering the entire droplet area for plasma formation. For the experiments performed at the out-of-focus configuration, analysis of Cu (I) signal at 324.75 nm indicated more than 7 times enhancement in *S*/*N* compared to the one obtained from the minimum focus experiments. Calibration graphs were constructed and LOD values were calculated for each element from their respective LIBS measurements. Absolute detection of 1.3 pg Cu, 3.3 pg Mn, 79 pg Cd and 48 pg Pb were achieved. The enhancements observed in signal intensities and better LODs may be attributed to the physical/chemical properties of 300 nm oxide grown silicon wafer ($Si+SiO_2$) substrate, in which a higher surface area is available for immobilization of metal ions. In addition, use of a relatively larger laser spot size at the out-of-focus condition provides increased interaction area with the target, therefore, larger plasma sizes and hence increased signal intensities are observed. ($Si+SiO_2$) substrate has also some advantages compared to other wood or graphite type substrates due to the absence of impurities of some metal elements. Compared to Si wafer substrate, ($Si+SiO_2$) substrate gives better results with a higher reproducibility (data are not presented here). LIBS analysis of CRM-TMDW reference samples has shown minimum 92% accuracy with relative standard deviations of at most 20%.

Direct analysis of nanoliters volume of droplets after drying on ($Si+SiO_2$) substrate by LIBS is a promising methodology that allows fast, simple, cheap and multielement analysis. It has also the potential to identify toxic elements on site that enables immediate action to be taken in the case of an environmental risk. Understanding and characterization of substrate effects in droplet analysis is a subject for more comprehensive work and currently under study in our laboratory.

Acknowledgments

Authors acknowledge, Izmir Institute of Technology through research grant 2014-İYTE-31 and IYTE-MAM staff for SEM pictures and EDX analyses.

References

[1] L.J. Radziemski, D.A. Cremers, Handbook of Laser Induced Breakdown Spectroscopy, John Wiley & Sons, West Sussex, England, 2006.
[2] A.W. Miziolek, V. Palleschi, I. Schechter, Laser Induced Breakdown Spectroscopy, Cambridge University Press, 2006.
[3] A. Kumar, F.Y. Yueh, J.P. Singh, Double-pulse laser-induced breakdown spectroscopy with liquid jets of different thicknesses, Appl. Opt. 4230 (2003) 6047–6051.
[4] Y. Feng, J. Yang, J. Fan, G. Yao, X. Ji, X. Zhang, X. Zheng, Z. Cui, Investigation of laser-induced breakdown spectroscopy of a liquid jet, Appl. Opt. 4913 (2010) C70–C74.
[5] C. Haisch, J. Liermann, U. Panne, R. Niessner R, Characterization of colloidal particles by laser-induced plasma spectroscopy (LIPS), Anal. Chim. Acta 3461 (1997) 23–35.
[6] S. Koch, W. Garen, W. Neu, R. Reuter, Resonance fluorescence spectroscopy in laser-induced cavitation bubbles, Anal. BioAnal. Chem. 3852 (2006) 312–315.
[7] E.M. Cahoon, J.R. Almirall, Quantitative analysis of liquids from aerosols and microdrops using laser induced breakdown spectroscopy, Anal. Chem. 845 (2012) 2239–2244.
[8] C. Janzen, R. Fleige, R. Noll, H. Schwenke, W. Lahmann, J. Knoth, P. Beaven, E. Jantzen, A. Oest, P. Koke, Analysis of small droplets with a new detector for liquid chromatography based on laser-induced breakdown spectroscopy, Spectrochim. Acta Part B: At. Spectrosc. 607 (2005) 993–1001.
[9] L.J. Radziemski, T.R. Loree, D.A. Cremers, N.M. Hoffman, Time-resolved laser-induced breakdown spectrometry of aerosols, Anal. Chem. 558 (1983) 1246–1252.
[10] N. Aras, S.Ü. Yeşiller, D.A. Ateş, Ş. Yalçın, Ultrasonic nebulization-sample introduction system for quantitative analysis of liquid samples by laser-induced breakdown spectroscopy, Spectrochim. Acta Part B: At. Spectrosc. 74 (2012) 87–94.
[11] J.-S. Huang, C.-B. Ke, L.-S. Huang, K.-C. Lin, The correlation between ion production nd emission intensity in the laser-induced breakdown spectroscopy of liquid droplets, Spectrochim. Acta Part B: At. Spectrosc. 571 (2002) 35–48.
[12] J.-S. Huang, H.-T. Liu, K.-C. Lin, Laser-induced breakdown spectroscopy in analysis of Al 3+ liquid droplets: on-line preconcentration by use of flow-injection manifold, Anal. Chim. Acta 5812 (2007) 303–308.
[13] J. Cáceres, J.T. López, H. Telle, A.G. Ureña, Quantitative analysis of trace metal ions in ice using laser-induced breakdown spectroscopy, Spectrochim. Acta Part B: At. Spectrosc. 566 (2001) 831–838.
[14] H. Sobral, R. Sanginés, A. Trujillo-Vázquez, Detection of trace elements in ice and water by laser-induced breakdown spectroscopy, Spectrochim. Acta Part B: At. Spectrosc. 78 (2012) 62–66.
[15] J. Simeonsson, L. Williamson, Characterization of laser induced breakdown

plasmas used for measurements of arsenic, antimony and selenium hydrides, Spectrochim. Acta Part B: At. Spectrosc. 669 (2011) 754–760.
[16] J.P. Singh, H. Zhang, F.-Y. Yueh, K.P. Carney, Investigation of the effects of atmospheric conditions on the quantification of metal hydrides using laser-induced breakdown spectroscopy, Appl. Spectrosc. 506 (1996) 764–773.
[17] S. Ünal, Ş. Yalçın, Development of a continuous flow hydride generation laser-induced breakdown spectroscopic system: Determination of tin in aqueous environments, Spectrochim. Acta Part B: At. Spectrosc. 658 (2010) 750–757.
[18] S.Ü. Yeşiller, Ş. Yalçın, Optimization of chemical and instrumental parameters in hydride generation laser-induced breakdown spectrometry for the determination of arsenic, antimony, lead and germanium in aqueous samples, Anal. Chim. Acta 770 (2013) 7–17.
[19] Z. Chen, H. Li, M. Liu, R. Li, Fast and sensitive trace metal analysis in aqueous solutions by laser-induced breakdown spectroscopy using wood slice substrates, Spectrochim. Acta Part B: At. Spectrosc. 631 (2008) 64–68.
[20] A. Sarkar, S.K. Aggarwal, K. Sasibhusan, D. Alamelu, Determination of sub—ppm levels of boron in ground water samples by laser induced breakdown spectroscopy, Microchim. Acta 168 (2010) 65–69.
[21] D.D. Pace, C. D'Angelo, D. Bertuccelli, G. Bertuccelli, Analysis of heavy metals in liquids using laser induced breakdown spectroscopy by liquid-to-solid matrix conversion, Spectrochim. Acta Part B: At. Spectrosc. 618 (2006) 929–933.
[22] D. Zhu, J. Chen, J. Lu, X. Ni, Laser-induced breakdown spectroscopy for determination of trace metals in aqueous solution using bamboo charcoal as a solid-phase extraction adsorben, Anal. Methods 43 (2012) 819–823.
[23] X. Wang, L. Shi, Q. Lin, X. Zhu, Y. Duan, Simultaneous and sensitive analysis of Ag (i), Mn (ii), and Cr (iii) in aqueous solution by LIBS combined with dispersive solid phase micro-extraction using nano-graphite as an adsorbent, J. Anal. At. Spectrom. 296 (2014) 1098–1104.
[24] D. Brouard, J.-F.Y. Gravel, M.L. Viger, D. Boudreau, Use of sol–gels as solid matrixes for laser-induced breakdown spectroscopy, Spectrochim. Acta Part B: At. Spectrosc. 6212 (2007) 1361–1369.
[25] D.A. Cremers, L.J. Radziemski, T.R. Loree, Spectrochemical analysis of liquids using the laser spark, Appl. Spectrosc. 385 (1984) 721–729.
[26] W. Pearman, J. Scaffidi, S.M. Angel, Dual-pulse laser-induced breakdown spectroscopy in bulk aqueous solution with an orthogonal beam geometry, Appl. Opt. 4230 (2003) 6085–6093.
[27] V.N. Rai, F.Y. Yueh, J.P. Singh, Time-dependent single and double pulse laser-induced breakdown spectroscopy of chromium in liquid, Appl. Opt. 4731 (2008) G21–G29.
[28] D.-H. Lee, S.-C. Han, T.-H. Kim, J.-I. Yun, Highly sensitive analysis of boron and lithium in aqueous solution using dual-pulse laser-induced breakdown spectroscopy, Anal. Chem. 8324 (2011) 9456–9461.
[29] K. Rifai, S. Laville, F. Vidal, M. Sabsabi, M. Chaker, Quantitative analysis of metallic traces in water-based liquids by UV-IR double-pulse laser-induced breakdown spectroscopy, J. Anal. At. Spectrom. 272 (2012) 276–283.
[30] A.C. Samuels, F.C. DeLucia, K.L. McNesby, A.W. Miziolek, Laser-induced breakdown spectroscopy of bacterial spores, molds, pollens, and protein: initial studies of discrimination potential, Appl. Opt. 4230 (2003) 6205–6209.
[31] X. Yu, Y. Li, X. Gu, J. Bao, H. Yang, L. Sun, Laser-induced breakdown spectroscopy application in environmental monitoring of water quality: a review, Environ. Monit. Assess. 18612 (2014) 8969–8980.
[32] K.M. Santos, J. Cortez, I.M. Raimundo, C. Pasquini, E.S.B. Morte, M.G.A. Korn, An assessment of the applicability of the use of a plasticised PVC membrane containing pyrochatecol violet complexing reagent for the determination of Cu^{2+} ions in aqueous solutions by LIBS, Microchem. J. 110 (2013) 435–438.
[33] Q. Shi, G. Niu, Q. Lin, X. Wang, J. Wang, F. Bian, Y. Duan, Exploration of a 3D nano-channel porous membrane material combined with laser-induced breakdown spectrometry for fast and sensitive heavy metal detection of solution samples, J. Anal. At. Spectrom. 2912 (2014) 2302–2308.
[34] M. Aguirre, S. Legnaioli, F. Almodóvar, M. Hidalgo, V. Palleschi, A. Canals, Elemental analysis by surface-enhanced laser-induced breakdown spectroscopy combined with liquid–liquid microextraction, Spectrochim. Acta Part B: At. Spectrosc. 79 (2013) 88–93.
[35] M. Aguirre, H. Nikolova, M. Hidalgo, A. Canals, Hyphenation of single-drop microextraction with laser-induced breakdown spectrometry for trace analysis in liquid samples: a viability study, Anal. Methods 73 (2015) 877–883.
[36] M. Aguirre, E. Selva, M. Hidalgo, A. Canals, Dispersive liquid–liquid microextraction for metals enrichment: a useful strategy for improving sensitivity of laser-induced breakdown spectroscopy in liquid samples analysis, Talanta 131 (2015) 348–353.
[37] A.M. de Jesus, M.Á. Aguirre, M. Hidalgo, A. Canals, E.R. Pereira-Filho, The determination of V and Mo by dispersive liquid–liquid microextraction (DLLME) combined with laser-induced breakdown spectroscopy (LIBS), J. Anal. At. Spectrom. 2910 (2014) 1813–1818.
[38] X. Wang, Y. Wei, Q. Lin, J. Zhang, Y. Duan, A simple, fast matrix conversion and membrane separation method for ultrasensitive metal detection in aqueous samples by laser induced breakdown spectroscopy, Anal. Chem. 87 (2015) 5577–5583.
[39] A. Metzinger, É. Kovács-Széles, I. Almási, G. Galbács, An assessment of the potential of laser-induced breakdown spectroscopy (LIBS) for the analysis of cesium in liquid samples of biological origin, Appl. Spectrosc. 687 (2014) 789–793.
[40] R. Wisbrun, I. Schechter, R. Niessner, H. Schroeder, K.L. Kompa, Detector for trace elemental analysis of solid environmental samples by laser plasma spectroscopy, Anal. Chem. 6618 (1994) 2964–2975.
[41] R.A. Multari, L.E. Foster, D.A. Cremers, Effect of sampling geometry on elemental emissions in laser-induced breakdown spectroscopy, Appl. Spectrosc. 50 (1996) 1483–1499.